

Experimental setup to study vibration spectra of hydrides of Group IV–VI elements in the liquid phase and liquefied gas solutions

Sh.Sh. Nabiev¹ and P.G. Sennikov²

¹ Russian Scientific Center "Kurchatov Institute," Moscow

² Institute of Chemistry of High-Purity Substances of the Russian Academy of Sciences, Nizhni Novgorod

Received July 1, 1999

A specialized experimental setup is described for investigation of vibration spectra of thermally stable volatile inorganic hydrides of Group IV–VI elements in the liquid phase and in liquefied gas solutions. Methods are proposed for measuring the concentration and integral absorption coefficients of the solutes. The results of investigation of vibration spectra of volatile inorganic hydrides (SiH₄, GeH₄, NH₃, PH₃, AsH₃, H₂S, and H₂Se) in the liquid phase and in cryogenic solutions are presented. Basic mechanisms of intermolecular interactions in these liquids are discussed based on the data on the strength, frequency, and profiles of vibrational bands.

1. Introduction

Volatile inorganic hydrides of Group IV–VI elements belonging to the 3rd to 5th periods of the periodic system have long been known to specialists in physics and chemistry. Under standard conditions these elements are, as a rule, chemically active, toxic, and explosive gases, which easily interact with oxygen and atmospheric moisture. These compounds are widely used for production of high-purity substances and important industrial isotopes, synthesis of optical materials, growing and doping of semiconducting epitaxial layers, etc.^{1,2} Recently, these compounds and their hydroxyl donor–acceptor complexes have become the subject of particular interest in atmospheric physics, because they can play an important role in optical radiation attenuation and affect photochemical reactions in the atmosphere.³

Investigation of vibration spectra of hydrides goes back to the 30s.⁴ Interest in their optical and spectroscopic properties has quickened in the last two decades. This is connected, on the one hand, with appearance of principally new methods of investigation, which allow refining some fundamental molecular characteristics, and, on the other hand, with the above-mentioned practical applications of these compounds since vibrational spectroscopy came into wide use in determining the degree of purity of hydrides and in studying the mechanisms of reactions with their participation.

Many papers are devoted to analysis of the vibration spectra of hydrides in the gas phase.^{5–7} However, the presence of hot bands and complex rotational–vibrational structure hinders adequate assignment of absorption bands in vibration spectra and, particularly, determination of the most important parameters of these bands, i.e., integral absorption

coefficients. Investigation of hydrides in the liquid phase and in gas solutions at low temperatures allows one to overcome, to a great extent, the above-mentioned difficulties.^{8,9} Note that until the mid-80s, studies of the vibration spectra of volatile hydrides in the liquid phase were almost absent. Whereas such data allow obtaining important information about structural features and dynamics of interacting molecules, as well as the character of intermolecular interactions.

This paper considers the basic elements of a specialized experimental setup, as well as the methods of measuring concentrations and integral absorption coefficients of solutes. Some results obtained for the last 15 years in investigation of the vibration spectra of the volatile inorganic Group IV–VI hydrides in the liquid phase and in solutions of liquefied gases are presented.

2. Basic applications of cryogenic spectroscopy

A comprehensive examination of vibration spectra of polyatomic molecules and weak molecular complexes with their participation requires dealing with low temperatures, what has been realized, for example, in the method of matrix isolation.^{10,11} However, this method has some limitations because of matrix splitting of the absorption bands and impossibility to determine the integral absorption coefficients, as well as to study combination and overtone bands and thermodynamic regularities of physical and chemical processes.

Solutions of the molecules under examination in liquefied gases at low temperatures open wider possibilities for obtaining voluminous information on their vibration spectra.⁹ The corresponding technique, which has been developed in scientific centers all over the world since the mid-70s, is currently known as

cryospectroscopy. Liquefied noble gases possessing high inertness and transparency to radiation from the vacuum ultraviolet to radiofrequency spectral region, as well as liquefied O₂ and N₂ having weak absorption bands in the mid-IR ($\approx 1550\text{ cm}^{-1}$ for O₂, and $\approx 2350\text{ cm}^{-1}$ for N₂) can be applied as solvents. This allows a significant increase in the accuracy of determination of vibrational frequency due to efficient suppression of rotational structure and disappearance of hot bands. Therewith, because of high density of a cryogenic solution, its spectrum in a meter layer is equivalent by sensitivity to that of the gas phase in a kilometer layer at the atmospheric pressure.

The main fields of applications of the cryospectroscopy are the following:

- obtaining of accurate information on frequencies and strengths of vibrational spectral bands of polyatomic molecules, including poorly known high-overtone transitions with $\Delta v = 4 - 6$. This information serves as the initial one for correct formulation of the electrooptical problem;

- detection of intermediate products of photochemical reactions and study of conformational equilibrium at low temperature;

- study of earlier unknown unstable molecular complexes;

- investigation of phase equilibrium in order to determine the solubility of different organic and inorganic compounds in liquefied gases;

- analysis of liquefied gases and some solutes for molecular impurities.

The relatively weak solubility of some molecular compounds in liquefied gases is a principal limitation of the cryospectroscopy. The liquefied gases at the atmospheric pressure are characterized by narrow temperature range of their liquid state which can be widened by increasing the pressure of the vapor above the liquid (Table 1). However, when using low-temperature cells allowing operation at pressures up to 40–50 atm, sufficiently wide temperature range can be obtained for each liquefied gas.

Table 1. Fundamental physical constants of liquefied gases

Property	Ar	Kr	Xe	O ₂	N ₂
T_{melt} , K	83.8	115.8	161.4	54.5	63.2
T_{boil} , K	87.3	119.8	165.0	90.2	77.4
T_{cr} , K	150.9	209.4	289.8	154.6	126.2
P_{cr} , atm	48.3	54.2	57.4	50.8	33.6
$V_m(T_{\text{boil}})$, cm ³ ·mol ⁻¹	28.7	43.7	49.9	28.0	34.9

We used cryospectroscopy in its traditional variant (investigation of solutions of substances in liquefied gases) for determination of the integral absorption coefficients for transitions with large Δv . Experimental equipment used for this purpose allows also examination of volatile compounds in the liquid phase at low temperature, what provides information on the structure of the liquid and the character of intermolecular interactions. Fundamental physical-

chemical constants of some volatile hydrides are presented in Table 2. As is seen, these compounds also have the narrow temperature range of the liquid state at the atmospheric pressure. Therefore, the use of cells withstanding the pressure up to 50 atm provides the possibility to study the vibration spectra of volatile hydrides in the liquid state from the boiling temperature T_{boil} up to 300 K (Ref. 12).

Table 2. Physical-chemical properties of some Group IV–VI hydrides

Property	SiH ₄	NH ₃	PH ₃	AsH ₃	H ₂ S	H ₂ Se
T_{melt} , K	88.5	195.4	139.35	156.23	187.63	207.43
T_{boil} , K	161.5	239.7	187.16	219.69	212.96	231.9
T_{cr} , K	269.4	405.6	324.54	374.5	373.6	410.6
ΔH_{melt} , kcal·mol ⁻¹	0.159	1.352	0.270	0.286	0.568	0.601
ΔH_{boil} , kcal·mol ⁻¹	2.687	5.581	3.362	3.798	4.483	4.64
P_{cr} , atm	41.7	112.0	59.0	65.8	78.6	83.9
$V_m(T_{\text{cr}})$, cm ³ ·mol ⁻¹	136.8	72.64	113.33	134.9	99.7	115.2
$V_m(T_{\text{boil}})$, cm ³ ·mol ⁻¹	54.9	24.85	45.9	47.7	36.2	41.0
$P_{300\text{ K}}$, atm	–	10.6	32.1	15.4	20.5	10.4

Investigation of the vibration spectra of the volatile hydrides requires development of specialized experimental equipment. In the following sections we discuss characteristics of different cryostats and cells, systems of gas filling and purification, as well as different methodical aspects of spectral analysis in liquids and cryogenic solutions and solubility calculation.

3. Design of optical cells and cryostats

The specificity of the problems under consideration determines the design of the cells and cryostats. High reactivity, toxicity, and explosion hazard of the hydrides impose drastic requirements upon the materials of the cells, cryostats, and optical elements should be made of. Their construction must be sufficiently flexible to can be quickly changed from the millimeter optical length (spectra of liquid hydrides) to the meter one (spectra of hydrides solved in liquid noble gases).¹²

We used the cryostat, which was a modification of that described in Ref. 13 (Fig. 1). All the parts to be in contact with the samples under investigation were made of stainless steel. The massive copper radiator 2, which was fixed on the cup for liquid nitrogen 3, housed the optical cell 1. The heater 4 was set in the bottom of the copper radiator. The cell temperature was controlled within the range from 80 to 300 K with a copper-constantan thermocouple. The accuracy of temperature determination was ± 1 K. To prevent freezing of cell windows, the system was put into the vacuum jacket 5. The windows 6 made of CaF₂ or KBr were fixed on the outer side of the vacuum jacket. Filling the cryostat with the gas to be studied and pumping it off were performed through the valves 7 and 8 and the feeding line 9 made of a stainless steel tube.

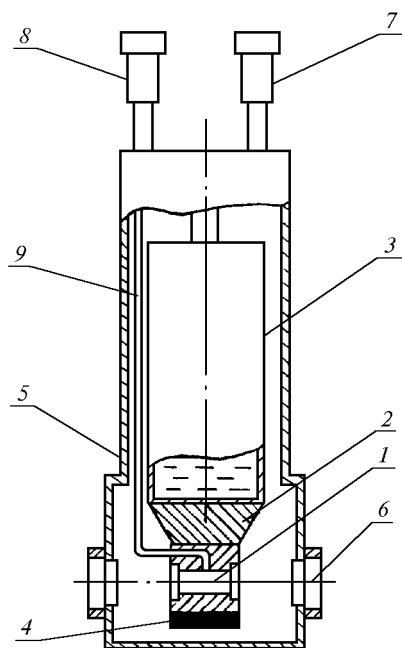


Fig. 1. Optical cryostat: cell (1), radiator (2), cup for liquid nitrogen (3), heater (4), vacuum jacket (5), windows (6), valves (7 and 8), and feeding line (9).

For studying the integral absorption coefficients of fundamental bands of the hydrides in solutions of liquefied gases, we used the cryostat cells allowing investigation of one and the same sample in two layers different by an order of magnitude. To measure the integral absorption coefficients of the combination and overtone bands, we used the cryostats based on the White scheme with a 10-cm-long base. It allows optical path tuning from the minimum (23 cm) to maximum (164 cm) length by rotating the plane illuminating mirrors outside the cell.¹²⁻¹⁴

For recording Raman spectra, samples with liquid hydrides were put into the cryostat of special design, the constructive feature of which, as compared to that intended for investigation of the IR spectra (see Fig. 1), was additional end windows 25 cm in diameter arranged in parallel with the exciting radiation. The distance between two other windows 15 mm in diameter was 100 mm. The cryostat was made of stainless steel too. The cell windows were made of sapphire, CaF_2 , BaF_2 , or ZnSe .

4. Method of mixture preparation

Figure 2 shows the system for preparation of cryogenic solutions based on liquefied noble gases.^{15,16} It consists of the system for preparing the mixtures to be examined and filling the cell with them, the system for purification of gases before their liquefaction, as well as for their purification after removal of the solution from the cell, and the instrumentation for temperature and pressure measurement and control.

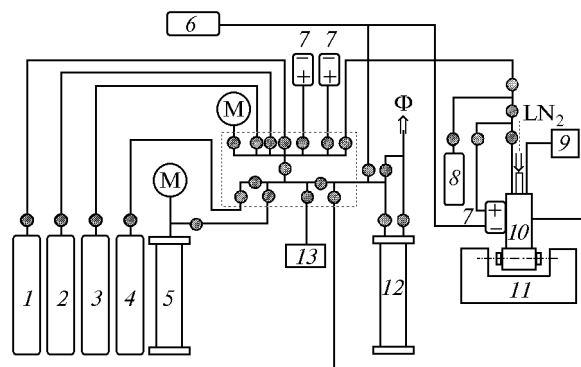


Fig. 2. Block diagram of the experimental cryospectroscopy setup: cylinders with noble gases (1-3), cylinders with hydrogen or fluorine (4), receiver (5), buffer volume (6), pressure indicator (7), cylinders with the gas under study (8), temperature indicator (9), optical cryostat (10), IR spectrophotometer (11), chemical absorber (12), gas cell (13), manometers (M), pump system (t), valves (v).

We used two methods to prepare cryogenic solutions^{7,15}:

- freezing-out of a pure substance into the cell with further condensation of the corresponding solvent gas;
- condensation of the prepared gas mixture of the substance under study (or several substances) with the solvent gas into the cell.

In measuring the spectral band strengths, we must take into account possible losses of substances in the feeding lines, as well as gas adsorption on the walls of metal vessels and desorption under the effect of gases entering the cell at high pressure. For each particular substance the procedure was developed for preparation of a mixture with a given concentration and quantitative estimation of the solution composition taking into account the physical-chemical properties of the substance. The accuracy of determination of the substance concentration in liquefied gas solutions was 5-10%.

Since in most cases we deal with measurements of very weak bands, purification of gases used as solvents (Ar , Kr , Xe , N_2 , O_2) is of prime importance. Although we used very pure gases, absorption bands of some impurities were recorded with a layer about tens centimeter thick. Therefore, additional purification of the gases was carried out during the measurement process. The gases were dehumidified by passage at high pressure through columns filled with zeolites of different types, KOH , and P_2O_5 or by cryofiltration.

5. Method for determination of the integral absorption coefficients and concentration of solutes

For measuring the IR absorption, the Bouguer-Lambert-Beer law is used. According to this law, the IR radiation flux at the frequency ν having passed through the sample under examination is

$$I(v) = I_0(v) \exp [-k(v) C l], \quad (1)$$

where I_0 is the IR radiation flux incident onto the sample, C is the concentration of absorbing molecules in the sample, l is the optical path length in the sample, and $k(v)$ is the absorption coefficient.

In the case of solutions Eq. (1) takes the form

$$I(v) = I_0(v) \exp \{- [c_1 k_1(v) + c_2 k_2(v)] l\}, \quad (2)$$

where k_1 and k_2 are the absorption coefficients, c_1 and c_2 are the solute and solvent concentrations, respectively. To characterize the absorption band strengths, the integral absorption coefficient

$$A = (1/c l) \int_{\nu_1}^{\nu_2} \ln I_0/I \, d\nu/\nu = \int_{\nu_1}^{\nu_2} k(v) \, d\nu \quad (3)$$

is used along with the absorption coefficient. The integration limits in Eq. (3) encompass the region of the absorption band under examination. The use of the integral absorption coefficients in description of the IR absorption is more convenient, because they are less sensitive to instrumental errors and conditions of spectrum recording as compared to the extinction coefficient. This is very important when dealing with cryogenic solutions, because IR absorption bands are narrow due to the low temperature and can be recorded with considerable errors. The optical density in the center of an absorption band strongly depends on the temperature at the constant substance concentration in the solution, while the integral band strength remains practically unchanged. Therefore, we rewrite Eq. (3) in the more convenient form

$$A = (cVB)/(N_A l x), \quad (4)$$

where A is the integral absorption coefficient of the sample ($\text{cm}^2 \cdot \text{molec}^{-1} \cdot \text{s}^{-1}$), c is the speed of light ($\text{cm} \cdot \text{s}^{-1}$), V is the molar volume of the solvent ($\text{cm}^3 \cdot \text{mol}^{-1}$), B is the integral strength of the solute absorption band (cm^{-1}), N_A is the Avogadro number ($\text{molec} \cdot \text{mol}^{-1}$), l is the optical path length in the sample (cm), x is the solute concentration (molar part).

We used Eq. (4) to determine the integral absorption coefficient A both in liquid hydrides ($x = 1$ molar part) and in their solutions in liquefied gases. In the former case layers with a thickness of several microns were used, and in the latter case the layer thickness was from several millimeters to several tens of centimeters. The methods of calculating the parameters by Eq. (4) in these cases are different, so we consider them separately.

Measuring in thick optical layers ($l > 0.5 \text{ mm}$)

The integral strength of the band B can be calculated from the equation

$$A = \int_{\nu_1}^{\nu_2} \ln I_0/I \, d\nu, \quad (5)$$

where the integration domain covers the region of the band under investigation (for bands with the Lorentz shape this region is equal to $5\Delta\nu_{1/2}$, where $\Delta\nu_{1/2}$ is the band half-width⁸). The molar volume V determined from the experimental liquid density at temperatures from T_{melt} to $T = 300 \text{ K}$ is calculated by the Racket equation¹⁷

The integral absorption coefficients obtained from studying the spectra of liquids and cryogenic solutions were recalculated for a free molecule by the Polo–Wilson equation¹⁸

$$A_{\text{sol}} = [(n^2 + 2)^2/9n] A_{\text{gas}} = K(n) A_{\text{gas}}, \quad (6)$$

where n is the refractive index of the cryogenic solution determined for the yellow D -line of sodium at $T = 20^\circ\text{C}$. For example, for liquid Ar ($T \cong 90 \text{ K}$) $n = 1.23$, for Kr ($T \cong 130 \text{ K}$) $n = 1.29$, and for Xe ($T \cong 180 \text{ K}$) $n = 1.39$. The correcting factor $K(n)$ accounts for the set of factors connected mostly with the change in the field strength of the incident light wave in liquids and cryogenic solutions with respect to the vacuum.

Measuring in thin optical layers ($l < 100 \text{ }\mu\text{m}$)

Thin optical layers were used, as a rule, to determine the absorption coefficients of liquid hydrides. The contribution of multiple internal reflection into the error of determination of the integral band strength was estimated by the equation¹⁹:

$$P = I_0/I = 1 - 2r^2 \exp(-4\pi\nu lk) \cos(2\varphi + 4\pi\nu ln) + r^4 \exp t(-8\pi\nu lk); \quad (7)$$

$$r = \{[(n - n_w)^2 + k^2]/[(n + n_w)^2 + k^2]\}^{1/2},$$

$$\varphi = \tan^{-1} [(2n_w k^2)/(n - n_w + k^2)],$$

where ν is the frequency, l is the optical path length, n and n_w are, respectively, the refractive indices of the sample and the window, and k is the imaginary part of the refractive index.

For the integral absorption coefficient of a band determined by Eq. (4) in thin optical layers, we also took into account the contribution into the optical path length from window bending caused both by temperature compression of the materials of the cell and windows and by the pressure change in the cell.

The optical thickness l in thin-layer cells is usually measured by the interferometric method in the absence of absorption bands using the equation²⁰

$$l = (m/2n) (\nu_1 - \nu_2)^{-1}, \quad (8)$$

where m is the number of interference maxima or minima between frequencies ν_1 and ν_2 , and n is the refractive index of the medium between the windows. Taking into account bending of the windows, the length l was determined in the following way. After recording the hydride spectra in a chosen temperature

range, the cell was filled with helium ($n \cong 1$), and then its optical thickness was calculated by Eq. (8) at the same pressure and temperature as in the experiment with the hydrid. The total systematic error of determination of A by Eq. (4) in thin optical layers did not exceed 20%.

6. Method of resolution of complex vibrational band contours

Obtaining information on individual components in the IR and Raman spectra of systems with strong intermolecular interaction is a rather complicated problem. Nevertheless, we resolved the experimental contours of vibrational bands of hydrids into elementary components by the method from Refs. 21 and 22. The approximating function is assumed therewith $y = f(\bar{x}, \nu)$, where the vector \bar{x} is a set of the parameters to be determined: $\bar{x} = \{x_n\}$ ($n = 1, 2, 3, \dots, N$). Mathematically, the task was to find \bar{x} minimizing the expression

$$\sigma^2 = (K - N)^{-1} \sum_{k=1}^K C_k^2 [I_k - f(\bar{x}, \nu)]^2,$$

where k is the number of the frequency ν_k at which the intensity of the absorbed (or scattered) radiation I_k in the vibration spectra ($k = 1, 2, 3, \dots$) was measured; C_k is the parameter characterizing the measurement accuracy; $K-N$ is the number of degrees of freedom. The function $f(\bar{x}, \nu)$ takes the form

$$f(\bar{x}, \nu) = \sum_{m=1}^M \varphi_m(\bar{x}, \nu) = x_{3m-2} [1 + (\nu - x_{3m-1})/x_{3m}]^{-1}.$$

The basis line roughly taking into account the background absorption (or scattering) was approximated by a polynomial of the second degree. We used the Fisher criterion to estimate the reliability of resolution of the spectrum.

It is important to note that the problem of resolution of an experimental spectrum with a complex structure into elementary spectra (which are its additive components) can be solved relatively simply with the use of the well-known mathematical methods.²¹ But, evidently, this problem should be solved only in the case that physical causes determining the contour shape are known (especially, in the case of complex contours with poorly pronounced maxima). Otherwise, the problem of resolution becomes purely mathematical. This means that one and the same contour may be approximated by different number of components (depending on peculiarities of a particular resolution algorithm), and it is practically impossible to assign some physical meaning to them. The approximation accuracy therewith naturally increases with the increase of the supposed number of elementary components.

7. Results and discussion

Among the hydrids of Group IV elements, vibration spectra of methane and silane have received the most study.²³⁻²⁵ Germane is not adequately investigated yet.²⁶ The parameters of the IR spectral bands of gaseous SiH_4 and GeH_4 are presented in Table 3. The integral coefficients of the ν_3 and ν_4 fundamental vibrational bands were determined only in Refs. 27-30. Note that in the case of silane the results are contradictory. The values of the ν_3 band strength of germane obtained in those works agree well with each other and with the data of Ref. 31. It is seen that some excess of $A(\nu_3)$ over $A(\nu_4)$ takes place for germane, whereas for silane the data obtained by the two groups of authors in Refs. 28 and 30, and in Refs. 29 and 31 are contradictory, what is most likely connected with insufficient measurement accuracy of the absorption coefficients.

Table 3. Frequencies (ν , cm^{-1}), integral absorption coefficients ($A \cdot 10^8$, $\text{cm}^2 \cdot \text{molec}^{-1} \cdot \text{s}^{-1}$), and relative band strengths in the IR spectra of SiH_4 and GeH_4 in the gas phase

Vibrational band	SiH_4			GeH_4		
	ν	A	A_{rel}	ν	A	A_{rel}
ν_4	913	199,	1000	820	122,	810
		Ref. 28			Ref. 30	
		147,	920		140,	
ν_3	2191	151,	760	2114	150,	1000
		Ref. 28			Ref. 30	
		160,	1000		153,	
		Ref. 29		Ref. 31		
$\nu_2 + 2\nu_4$	—	—	—	—	—	—
$\nu_1 + \nu_4$	—	—	—	—	—	—
$\nu_3 + \nu_4$	3110	—	—	—	—	—
$\nu_2 + \nu_3$	3150	—	—	—	—	—
$2\nu_1$	4308	—	—	4154	—	—
$2\nu_3$	4379	—	—	—	—	—
$\nu_1 + \nu_3$	4309	—	—	—	—	—
$3\nu_1$	6362	—	—	—	—	—
$2\nu_1 + \nu_3$	—	—	—	—	—	—
$\nu_1 + 2\nu_3$	6496	—	—	—	—	—
$3\nu_3$	6000	—	—	—	—	—

The data on the IR spectra of gaseous silicon and germanium hydrids are well supplemented by the results obtained from investigation of the IR spectra of their solutions in liquefied noble gases.²⁶ Application of a multipass cell allowed Sennikov et al.²⁶ to assign, for the first time, numerous weak combination and overtone vibrational bands in the range from 900 to 6500 cm^{-1} up to transitions with $\Delta\nu = 3$ and to refine the strength ratio of the ν_3 and ν_4 bands in the spectra of silane and germane.

The IR absorption spectrum of liquid silane in the area of fundamental vibrations was first studied in Ref. 32 with the optical layer about 1 mm thick. In Ref. 33 the IR spectra of SiH_4 and GeH_4 in the liquid

phase were studied in the wider range from 800 to 5000 cm^{-1} (Table 4), but with a thicker optical layer. This is insufficient to obtain the information on temperature dependence of the frequency, shape, and strength of the fundamental bands.

Table 4. Frequencies (ν , cm^{-1}) of bands in the IR spectra of liquid SiH_4 and GeH_4

Vibrational band	SiH_4	GeH_4
	$T = 190 \text{ K}$	$T = 246 \text{ K}$
ν_4	910	$\cong 820$
$2\nu_4$	–	–
$\nu_2 + \nu_4$	1860	1730
ν_3	2200	$\cong 2100$
$3\nu_4$	2685	2415
$\nu_1 + \nu_4$	2837	2660
$\nu_3 + \nu_4$	3090	2910
$\nu_2 + \nu_3$	3130	–
$2\nu_2 + 2\nu_4$	–	–
$\nu_3 + 2\nu_4$	–	–
$\nu_2 + \nu_3 + \nu_4$	4040	3713
$\nu_1 + \nu_3$	–	–
$2\nu_3$	4295	4125

Similarly to the IR spectra, the Raman spectra of SiH_4 and GeH_4 were investigated in the gas (Refs. 34 and 35) and solid-state (Ref. 36) phases. The Raman spectra of liquid germane in the 200–300 K temperature range were studied systematically in Ref. 37. Table 5 shows that, similarly to the IR spectra, lines in the Raman spectra of liquid silane and germane, including the common line of stretching vibrations, which is the superposition of lines of the ν_1 and ν_3 bands unresolved under experimental conditions, suffer a noticeable long-wave shift at the gas–liquid transition. The only exception is the ν_4 band of germane; its maximum, to the contrary, shifts toward higher frequencies. The study of the temperature dependence of the Raman lines of liquid germane did not reveal noticeable shifts of their maxima.³⁷ Comparative analysis of the vibrational and rotational correlation functions and times of vibrational ($\tau_V = 1.5 \text{ ps}$) and orientational ($\tau_R = 4.5 \text{ ps}$) relaxation of the GeH_4 molecules in the liquid phase has shown that the values of τ_V and τ_R remain practically constant, and the germane molecules are involved in the rotational

motion, usual for liquid systems, and change their orientation as isolated kinetic particles. Their motion therewith is described by the model of the Debye type (small-angle rotational diffusion),^{9,38–40} and the elementary rotation angle of a germane molecule at the first step of diffusion is no more than 4–5°.

Table 5. Frequencies (ν , cm^{-1}) of fundamental bands in the Raman spectra of silane and germane in the gas and liquid phases

Vibrational band	SiH_4		GeH_4	
	Gas	Liquid	Gas	Liquid
	$T = 293 \text{ K}$	$T = 98 \text{ K}$	$T = 293 \text{ K}$	$T = 290 \text{ K}$
ν_1	2185.7		2110.6	
ν_3	2189.1	2171.0	2111.5	2091.5
ν_2	972.1	961.7	930.6	916.0
ν_4	913.3	–	821.0	826.2

Table 6 presents the parameters of the IR spectral bands of the hydrides of Group V elements in the gas and liquid phases.^{7,14} The IR spectra of these hydrides in the liquid phase at two different temperatures are shown in Figs. 3, 4, and 5. In the IR spectrum of NH_3 the ν_2 bending band is most intense, while in the spectra of analogous hydrides the ν_1 and ν_3 stretching bands are strongest. On the whole, the strength of the ν_1 and ν_3 bands grows from top to bottom of the group, while the strength of the ν_2 and ν_4 bands lowers. Based on the analysis of the obtained spectra of the hydrides of Group V elements, some more dissimilarities between NH_3 and its structural analogs in the group were found. The NH_3 stretching bands at the gas–liquid transition shift toward lower frequency, while the small high-frequency shift is typical of the bending vibrations. The integral absorption coefficient of the band of stretching vibrations on the whole (including the overlapping weak $2\nu_4$ overtone band) grows significantly at practically constant strengths of the ν_2 and ν_4 bands. The above-mentioned peculiarities practically do not manifest themselves in the spectra of liquid PH_3 and AsH_3 . The frequency and strength of their fundamental bands change only slightly at the gas–liquid transition (especially in the case of AsH_3).

Table 6. Temperature dependence of the frequency (ν_i , cm^{-1}) and integral absorption coefficients ($A \cdot 10^8 \text{ cm}^2 \cdot \text{molec.}^{-1} \cdot \text{s}^{-1}$) of the fundamental bands in the vibration spectra of the liquid PH_3 and AsH_3

T, K	PH_3								
	IR						Raman*		
	$\nu_{1,3}$	A	ν_2	A	ν_4	A	$\nu_{1,3}$	ν_2	ν_4
290	2314	72	999	11.3	1091	12.7	2307	974	1117
269	2314	72	999	10.6	1100	13.4	2306	975	1115
240	2314	73	997	10.3	1100	13.7	2306	977	1114
222	2313	74	995	10.2	1101	13.8	2305	978	1115
181	2312	75	990	10.0	1102	14.0	2304	981	1110

Table 6 (continued)

T, K	AsH ₃								
	IR						Raman		
	$\nu_{1,3}$	A	ν_2	A	ν_4	A	$\nu_{1,3}$	ν_2	ν_4
295	2115	128	906	10.8	976	16.1	2096	898	989
267	2113	134	903	13.7	977	13.3	2095	901	990
241	2109	125	906	14.0	978	13.2	2095	905	989
221	2107	121	905	14.7	976	13.3	2094	908	986
182	2104	118	904	15.5	977	13.5	2093	910	985

* Frequencies of lines in the VV-spectra are given.

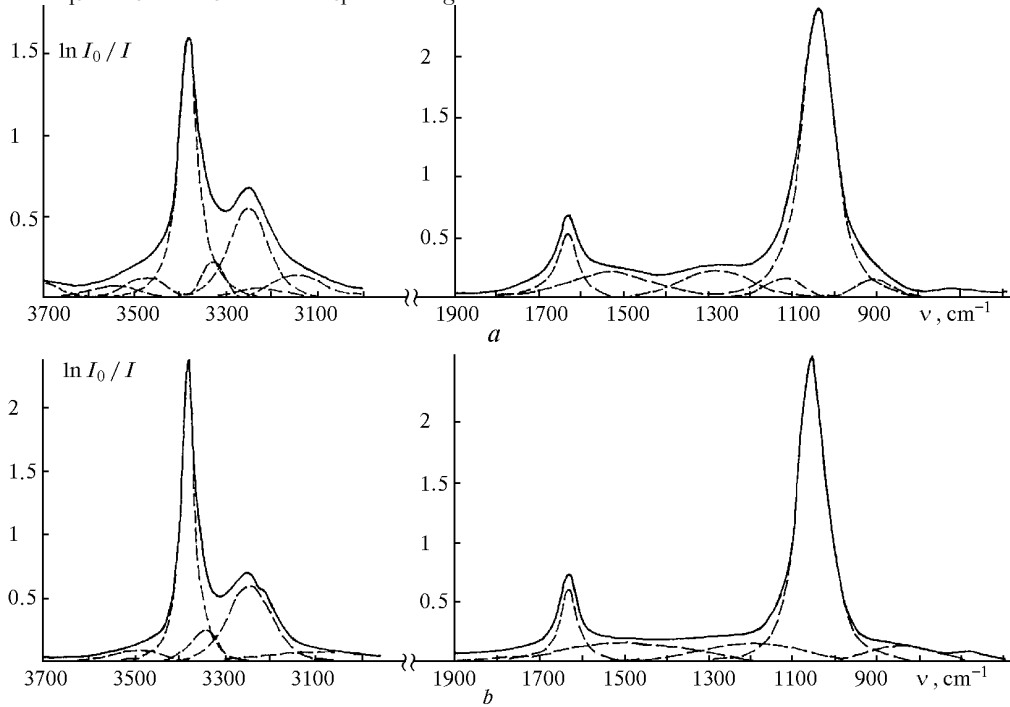


Fig. 3. IR absorption spectrum of liquid ammonia in the region of fundamental bands at 289 (a) and 198 K (b).

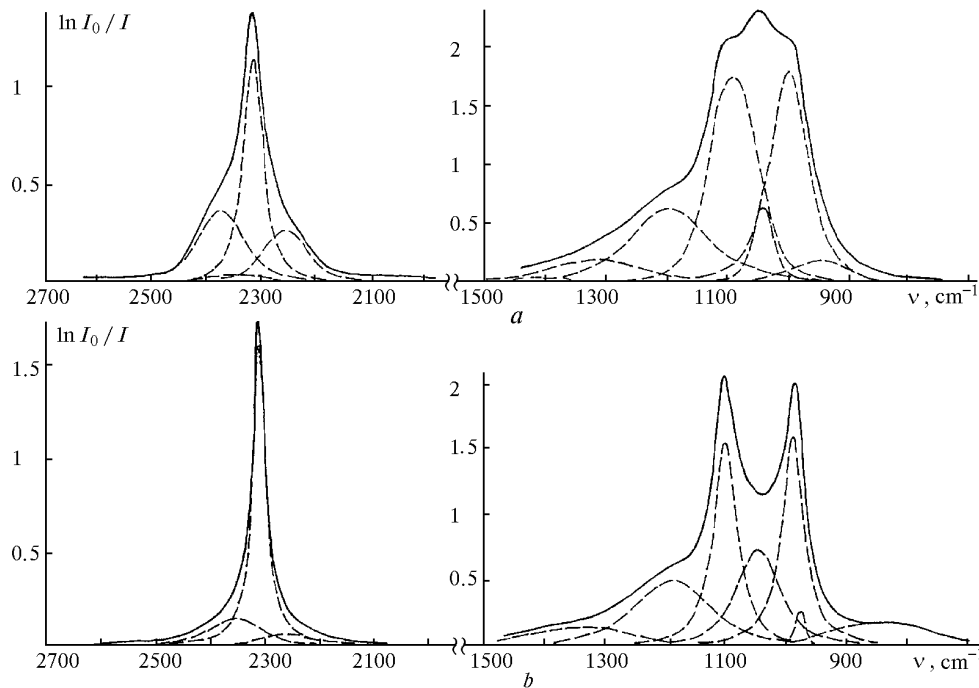


Fig. 4. IR absorption spectrum of liquid phosphine in the region of fundamental bands at 290 (a) and 153 K (b).

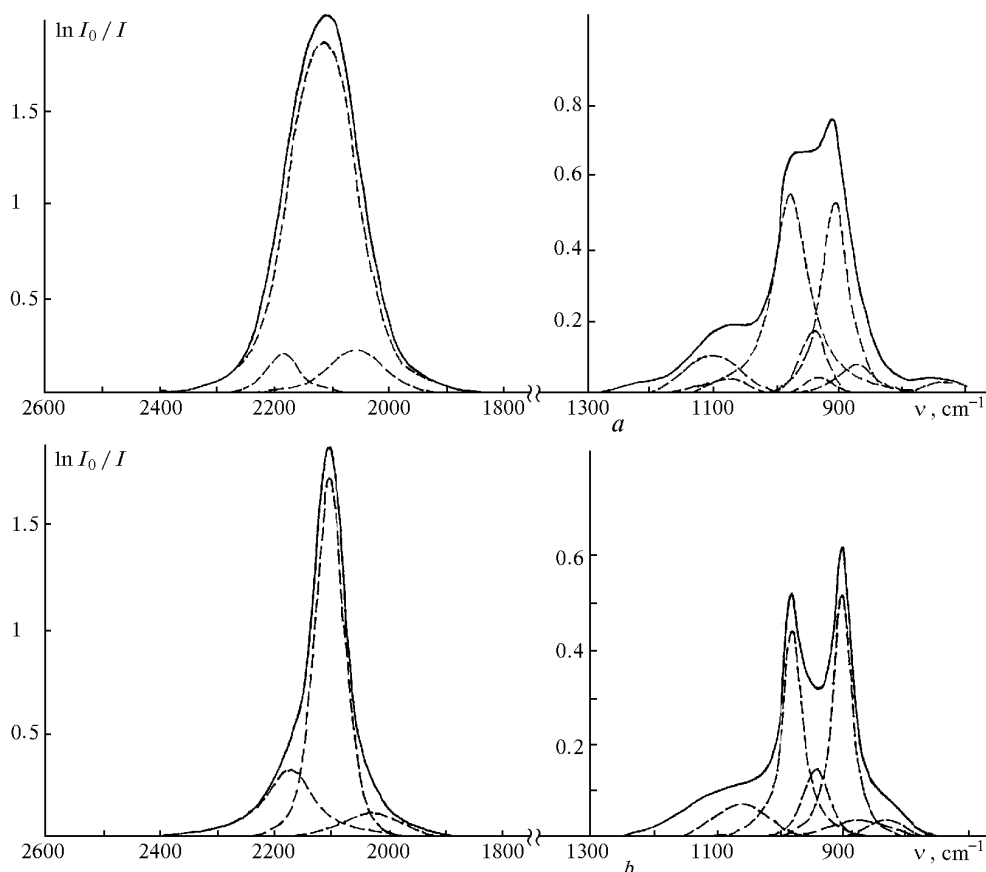


Fig. 5. IR absorption spectrum of liquid arsine in the region of fundamental bands at 295 (a) and 157 K (b).

The IR absorption spectra of liquid NH_3 , PH_3 , and AsH_3 in a wide temperature region (150–300 K) were investigated in detail in Refs. 21 and 22. The small low-frequency shift (4 cm^{-1}) of the ν_{str} band was observed in the spectrum of liquid NH_3 at low temperature. The peak of the ν_2 band noticeably shifts (by 13 cm^{-1}) toward higher frequency, while the position of the ν_4 band remains practically unchanged.

These tendencies are noticeably smoothed at transition from NH_3 to PH_3 . So, the position of the ν_{str} band is temperature independent. The ν_2 band shifts considerably (by 9 cm^{-1}) toward lower frequency, while the maximum of the ν_4 vibrational band shifts toward higher frequency (by 11 cm^{-1}) as the phosphine temperature decreases.

The situation changes drastically in the case of arsine. The change in the temperature of liquid AsH_3 leads to the significant (12 cm^{-1}) low-frequency shift of the ν_{str} band, while the frequencies of the ν_2 and ν_4 bending bands remains practically constant.

The differences between spectral characteristics of liquid NH_3 , PH_3 , and AsH_3 observed in Refs. 41 and 42 can be associated with different stability of local intermolecular interactions. The marked low-frequency shift ($> 40 \text{ cm}^{-1}$) of the ν_{str} band observed in case of NH_3 molecule at the gas-liquid transition, an increase of its integral strength in the liquid phase at temperature decrease, and the high-frequency shift of ν_{bend} band with the unchanged strength are typical of

systems with the hydrogen bond. These facts agree with the assumption of associative processes in gaseous and liquid NH_3 (Refs. 43 and 44) and can serve as a proof of formation of NH_3 pair associates in the liquid phase. The results of study of the IR spectra of hydrides of Group VA elements in solutions of noble gases^{7,14,16,45} also point to the formation of rather stable H-bond complexes in NH_3 . Unlike PH_3 and AsH_3 , whose solubility in liquid Ar ($T = 96 \pm 2 \text{ K}$) is $4.2 \cdot 10^{-1}$ and $2.8 \cdot 10^{-1} \text{ mol} \cdot \text{l}^{-1}$, respectively,^{7,16,45} NH_3 is almost insoluble in liquid Ar and Kr, what is typical of H_2O , as well as much less associated H_2S and H_2Se .

Enthalpy of intermolecular interactions in liquid NH_3 , PH_3 , and AsH_3 was estimated in Refs. 7 and 14 on the assumption that in liquid NH_3 , on the average, one H-bond occurs between two molecules. This assumption is even more obvious for liquid PH_3 and AsH_3 . The value $\Delta H_{290} = -1.7 \text{ kcal} \cdot \text{mol}^{-1}$ obtained from the IR spectra of liquid NH_3 well agrees with the results of quantum-chemistry calculation for the $(\text{NH}_3)_2$ dimer.⁴⁶ For liquid PH_3 , ΔH_{298} is estimated as $-0.1 \text{ kcal} \cdot \text{mol}^{-1}$, what also agrees well with the results of quantum-chemistry calculation for the $(\text{PH}_3)_2$ dimer, namely, $\Delta H_{298} = -0.3 \text{ kcal} \cdot \text{mol}^{-1}$ (Ref. 47). The value of ΔH_{298} for liquid AsH_3 is almost equal to zero.

Table 7 presents the times of vibrational (τ_V) and orientational (τ_R) relaxation of the PH_3 and AsH_3 molecules calculated from the contour of the ν_2 line in the Raman spectrum according to Refs. 9, 38, and 39.

Table 7. Frequencies (ν , cm^{-1}), half-widths (c , cm^{-1}), differences between maxima ($\delta\nu$, cm^{-1}) of the ν_2 (A_1) line in the isotropic and anisotropic Raman spectra of liquid hydrides, and the times of vibrational (τ_V , ps) and orientational (τ_R , ps) relaxation of PH_3 and AsH_3 at various temperatures

Hydrid	T , K	ν_{iso}	Γ_{iso}	ν_{aniso}	Γ_{aniso}	$\delta\nu = \nu_{\text{aniso}} - \nu_{\text{iso}}$	τ_V	τ_R
PH_3	290	974.4	18.3	974.7	22.2	0.3	1.15 ± 0.10	3.25 ± 0.20
	269	975.7	17.0	976.1	18.9	0.4	1.30 ± 0.10	4.72 ± 0.15
	240	977.6	16.2	978.5	17.8	0.9	1.41 ± 0.07	6.10 ± 0.12
	222	980.1	15.7	981.4	17.2	1.3	1.40 ± 0.05	6.47 ± 0.10
	181	981.8	15.2	983.6	16.5	1.8	1.48 ± 0.05	7.42 ± 0.10
AsH_3	295	899.9	18.1	900.1	30.9	≈ 0.2	1.55 ± 0.10	0.40 ± 0.15
	267	903.2	17.1	902.3	26.7	-0.9	1.31 ± 0.07	0.68 ± 0.12
	241	906.1	16.9	902.8	23.8	-3.3	1.21 ± 0.06	1.50 ± 0.12
	221	908.7	15.0	904.6	17.3	-4.1	1.32 ± 0.05	3.05 ± 0.10
	182	911.8	14.6	906.2	15.9	-4.7	1.44 ± 0.05	4.75 ± 0.10

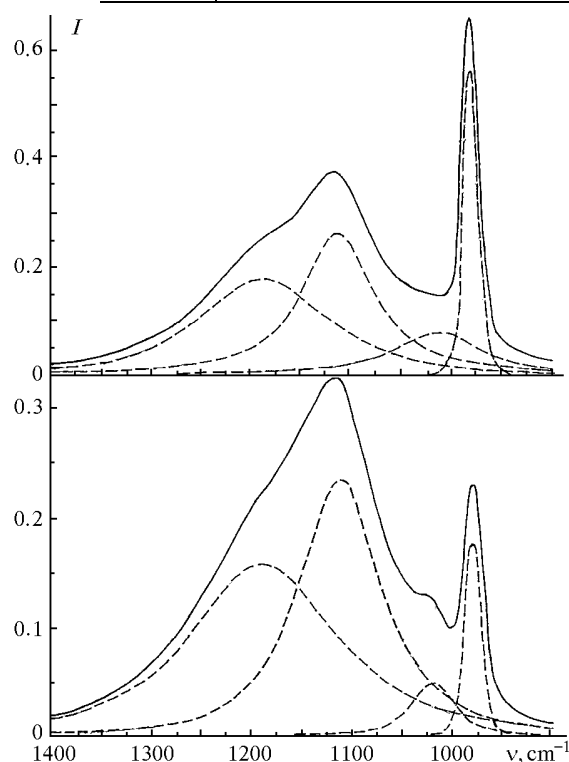


Fig. 6. Raman spectrum of liquid phosphine in the region of bending vibrations at two different polarizations ($T = 243$ K).

The shape of the Raman spectrum of liquid phosphine in the range of bending vibrations is shown in Fig. 6 for two different polarizations. Analysis of the time behavior of the obtained vibrational and rotational time correlation functions (TCF's), as well as the data from Table 7 have shown that τ_V weakly depends on the temperature of liquid PH_3 and AsH_3 and varies within 1.2–1.5 ps. At the same time, the temperature decrease of liquid hydrides from 295 to 181 K is accompanied by the noticeable increase of τ_R : from 3.1 to 7.4 (PH_3) and from 0.4 to 4.8 ps (AsH_3). In the case of AsH_3 , in contrast to PH_3 and most other molecules in liquid phase,^{9,38–40} the process of rotational relaxation contributes mostly into

formation of the ν_2 line contour at the room temperature. This may be caused by several circumstances. At high temperatures the PH_3 and AsH_3 molecules (as in the case of GeH_4) are involved in rotational motion, typical of non-associated liquid systems, and change their orientation as isolated kinetic particles. So their motion is also described by the model of the Debye type.⁹ As the temperature decreases, rotatability of the PH_3 and AsH_3 molecules decreases, what likely follows from the smaller number of collisions between particles in unit time due to the decrease of their angular rate and kinetic power, as well as intensification of intermolecular interactions. One of the most probable causes of the temperature dependence of τ_R in hydrides is the presence of associative processes in these liquids.

The values of the frequency and half-width of ν_2 in the isotropic and anisotropic Raman spectra of liquid PH_3 and AsH_3 at different temperatures are given in Table 7. They show that in the case of PH_3 the temperature decrease results in the “normal” ($\nu_{\text{iso}} < \nu_{\text{aniso}}$) effect at which $\delta\nu$ varies from 0.3 to 1.8 cm^{-1} . In the case of AsH_3 , to the contrary, the “abnormal” ($\nu_{\text{iso}} > \nu_{\text{aniso}}$) effect is observed. The temperature variation in arsine within practically the same range causes the variation of $\delta\nu$ from 0.2 to -4.7 cm^{-1} .

In contrast to many liquid systems, it is not reasonable to associate both the “normal” and “abnormal” effects in liquid hydrides with only the resonance exchange of vibrational energy. The discrepancy between the maxima of lines with a complex structure in the isotropic and anisotropic spectra may be also caused by different strength and degree of depolarization of elementary components and depends on the concentration of associates of different type. Although for most liquids the resonance exchange occurs mainly between associates of the same type, in the case of liquid hydrides the temperature decrease results in disturbance of the balance between different structure formations and, as a consequence, in the change of the strength and degree of depolarization of the corresponding components of the ν_2 line contour in the isotropic and anisotropic Raman

spectra. This does not contradict the idea developed recently in Ref. 48. Taking into account the presence of both "normal" (PH_3) and "abnormal" (AsH_3) effects in the Raman spectra of liquid hydrides, it counts in favor of the above assumptions on the different character of intermolecular interactions in the liquids considered. It should be noted that besides the above-mentioned causes, nonrigid intramolecular regrouping in associates of the $(\text{PH}_3)_2$ and $(\text{AsH}_3)_2$ type also can contribute significantly to $\delta\nu$.⁴⁹ By now it is still an open question which requires further investigation.

The transition from the hydride of the second period element (NH_3) to that of the third (PH_3) and fourth (AsH_3) period elements within the same group, on the one hand, should be accompanied by some decrease in the capability of molecules to form H-bonds, at least, because of the decrease in the electronegativity of the hydride-generating element. On the other hand, the energy of non-specific (Van der Waals) interaction for the above-stated reasons (for example, increase in polarizability) must increase at such a transition. Therefore, the low-frequency shift of ν_{str} in the IR spectrum of liquid arsine^{41,42} at the almost constant integral absorption coefficient, more than tenfold change of τ_R , and the significant "abnormal" effect of discrepancy between the ν_2 line maxima in the isotropic and anisotropic Raman spectra at the temperature decrease are connected, in our opinion, just with intensification of the Van der Waals interaction between AsH_3 molecules. Thus, the liquid hydrides of the Group VA elements can be ordered by the decrease in the energy of specific intermolecular interactions as follows: $\text{NH}_3 > \text{PH}_3 \geq \text{AsH}_3$.

The parameters of bands observed in the IR spectra of the hydrides of Group VI elements in the gas and liquid phases⁵⁰⁻⁵² are given in Table 8. The IR absorption spectra of liquid H_2S and H_2Se in the area of fundamental bands, as well as the contour of the first overtone $2\nu_{\text{str}}$ band at different temperature are shown in Figs. 7 and 8.

Table 8. Frequencies (ν , cm^{-1}), absolute ($A \cdot 10^8$, $\text{cm}^2 \cdot \text{molec}^{-1} \cdot \text{s}^{-1}$) and relative (A_{rel}) strengths of the absorption bands in the IR spectra of H_2S and H_2Se in the gas and liquid phases ($T = 293 \text{ K}$)

Type of vibrations	H_2S			H_2Se		
	ν	A	A_{rel}	ν	A	A_{rel}
Gas						
ν_1	2615			2345		
		0.06	25		6.5	100
ν_3	2625			2358		
ν_2	1183	0.24	—	1034	0.8	12
Liquid						
ν_{str}	2580	12.0	100	2305	14.0	100
ν_{bend}	1186	2.9	15.40	1030	2.4	17.1
$\nu_{\text{str}} + \nu_{\text{bend}}$	3757	1.4	10.8	3323	0.8	5.7
$2\nu_{\text{str}}$	≈ 5100	0.24	19	≈ 4530	1.0	7.2
$2\nu_{\text{str}} + \nu_{\text{bend}}$	≈ 6200	0.046	35	≈ 5540	0.02	14
$3\nu_{\text{str}}$	≈ 7500	0.006	5	≈ 6680	0.04	26
$3\nu_{\text{str}} + \nu_{\text{bend}}$	≈ 8590	0.002	1.5	≈ 7650	0.001	0.7
$4\nu_{\text{str}}$	—	—	—	≈ 8740	0.002	1.4

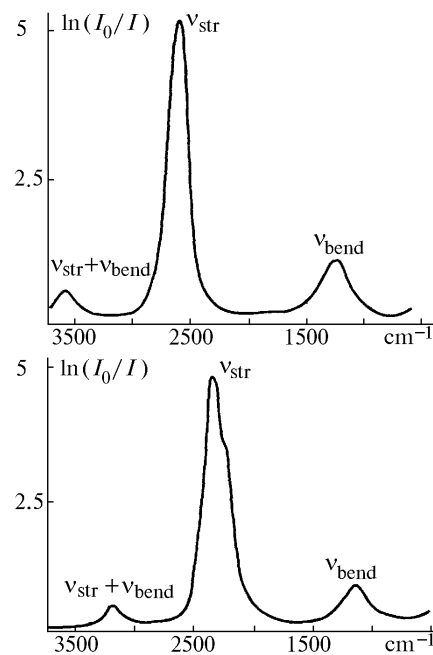


Fig. 7. IR absorption spectra of liquid hydrogen sulfide (a) and hydrogen selenide (b) in the region of fundamental bands at $T = 294$ and 293 K , respectively; $l = 0.1 \text{ mm}$.

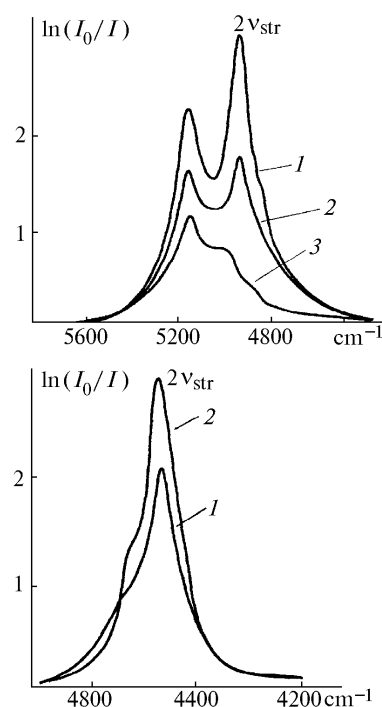


Fig. 8. IR absorption spectra of liquid hydrogen sulfide (a) and hydrogen selenide (b) in the region of $2\nu_{\text{str}}$ at the different temperature T : 199 (1), 247 (2), and 292 K (3), $l = 5 \text{ mm}$ (a); 213 (1) and 293 K (2); $l = 1.5 \text{ mm}$ (b).

The data for H_2S tabulated in Table 8 demonstrate a significant low-frequency shift of the ν_{str} band ($\Delta\nu \approx 34 \text{ cm}^{-1}$, $T = 292 \text{ K}$) and a high-frequency shift of the ν_{bend} band ($\Delta\nu \approx 50 \text{ cm}^{-1}$, $T = 292 \text{ K}$) at the gas-liquid transition. The position of the latter

significantly depends on the temperature, shifting toward lower frequencies as the temperature decreases. The temperature decrease leads to an increase in the integral absorption coefficient of the ν_{str} band in spectrum of liquid H_2S from $11.2 \cdot 10^{-8} \text{ cm}^2 \cdot \text{molec}^{-1} \cdot \text{s}^{-1}$ at 300 K to $18.1 \cdot 10^{-8} \text{ cm}^2 \cdot \text{molec}^{-1} \cdot \text{s}^{-1}$ at 180 K, while the value of A for the ν_{bend} band decreases a little.

For H_2Se the gas-liquid transition is accompanied by shift of ν_{str} toward lower frequency ($\Delta\nu \cong 40 \text{ cm}^{-1}$), while ν_{bend} remains practically unchanged. As the temperature decreases, the integral absorption coefficient of the ν_{str} band in the spectrum of liquid H_2Se slightly grows (from $14.6 \cdot 10^{-8} \text{ cm}^2 \cdot \text{molec}^{-1} \cdot \text{s}^{-1}$ at 295 K to $15.1 \cdot 10^{-8} \text{ cm}^2 \cdot \text{molec}^{-1} \cdot \text{s}^{-1}$ at 213 K).

It should be noted that the strength of the ν_{str} band of H_2S grows extremely (more than 200 times) at the gas-liquid transition (for H_2O it is an order of magnitude less). However, the sharp growth of the strength of the weak S-H bond in contrast to the gas phase does not mean the similar growth in the capability of H_2S to form associates at the gas-liquid transition, because the measure of the H-bond strength is not simply the change ΔA , but the value $\Delta A^{1/2} = \Delta A_{\text{bond}}^{1/2} - \Delta A_{\text{free}}^{1/2}$, where A_{free} and A_{bond} are the integral absorption coefficients of the AH groups in a free proton donor molecule and in the AH ... B complex, respectively.⁵³ The relation between the enthalpy of the hydrogen bond ΔH and $\Delta A^{1/2}$ can be written as⁵⁴:

$$\Delta m = -2.9 (A_{\text{bond}}^{1/2} - A_{\text{free}}^{1/2}). \quad (9)$$

Here Δm is in $\text{kcal} \cdot \text{mol}^{-1}$, and A is in $\text{cm} \cdot \text{mmol}^{-1}$. This rule holds for all known bonds of the X-H ... B type (X = O, N, C, S, etc) and covers all the classes of H-bonds in 1:1 complexes within the energy range of 0.1–15 $\text{kcal} \cdot \text{mol}^{-1}$ including pure associated liquids.

To estimate the enthalpy of the H-bond in liquid H_2S , we used Eq. (9) in the form⁵⁰:

$$-\Delta m = 2.9[(A_{\text{bond}}/m)^{1/2} - A_{\text{free}}^{1/2}], \quad (10)$$

where m is the number of hydrogen bonds, formed by the proton donor molecule. Based on the structure of the H_2S molecule, one could expect the value of m to vary within the limits $1 \leq m \leq 2$. The value $A_{\text{free}} = 0.0014 \cdot 10^4 \text{ cm} \cdot \text{mmol}^{-1}$ corresponds to the integral absorption coefficient of the $\nu_{1,3}(\text{SH})$ band in the gas phase accurate to the coefficient $L(n)$ (n is the H_2S refractive index) accounting for the change in the field strength of the light wave at the gas-liquid transition. The value $A_{\text{bond}} = 0.335 \cdot 10^4 \text{ cm} \cdot \text{mmol}^{-1}$ corresponds to the integral absorption coefficient of $\nu_{\text{str}}(\text{SH})$ in the liquid. In this case the enthalpy of the hydrogen bond SH ... S in liquid H_2S varies within $(-1.0) - (-1.6) \text{ kcal} \cdot \text{mol}^{-1}$ at $T_b = 213 \text{ K}$ depending on the structure of a hypothetical isolated associate.

By analogy with liquid water,⁵⁵ the equilibrium existing in liquid H_2S between proton-donor and proton-acceptor fragments of this molecule can be described by the following simple scheme:



The equilibrium constant for the processes of this type is

$$K = \frac{u_{\text{bond}}}{u_{\text{free}} X (:S_{\text{free}})} = \frac{u_{\text{bond}}}{u_{\text{free}}^2}, \quad (12)$$

where u_{bond} and u_{free} are the molar portions of “bonded” and “free” SH-groups determined from the Lambert-Beer equation. With these relations, we can estimate the mean value of the H-bonds formation enthalpy in liquid H_2S . It is equal to $(-1.5 \pm 0.2) \text{ kcal} \cdot \text{mol}^{-1}$ and agrees with the estimate of Δm obtained from the analysis of the ν_{str} band strength of liquid H_2S .

Analysis of the strength of components of the $2\nu_{\text{str}}$ band in the spectrum of liquid H_2S allowed determination of the portion of “bonded” and “free” S-H oscillators in the liquid phase and calculation of the integral absorption coefficients of the corresponding components of the stretching band in the IR spectrum of liquid H_2S : $A_{\text{free}}(\nu_{\text{str}}) = 0.12 \cdot 10^4 \text{ cm} \cdot \text{mmol}^{-1}$ and $A_{\text{bond}}(\nu_{\text{str}}) = 0.60 \cdot 10^4 \text{ cm} \cdot \text{mmol}^{-1}$. The value of the enthalpy for formation of H-bonds between molecules in liquid H_2S estimated by Eq. (12) falls in the interval $-\Delta m = 0.6 - 1.2 \text{ kcal} \cdot \text{mol}^{-1}$. This result well agrees with the quantum-chemistry calculation of the energy for formation of the $(\text{H}_2\text{S})_2$ dimer.⁴⁷ The enthalpy of the hydrogen bond in liquid H_2S can be estimated from below as $\Delta m = -0.6 \text{ kcal} \cdot \text{mol}^{-1}$.

Thus, the character of the IR spectra of liquid H_2S in the region of stretching vibrations and their first overtone is indicative of formation of H-bonds in liquid H_2S . However, these bonds are much weaker than those in liquid water. The portion of “free” H_2S molecules in the liquid phase at 290 K is about 75%.

Equation (9) remains the only possible estimate of the enthalpy of hydrogen bonds in liquid H_2Se because a significant portion of H_2Se molecules in the liquid phase evidently remains “free.” At $A_{\text{bond}} = 0.314 \cdot 10^4 \text{ cm} \cdot \text{mmol}^{-1}$ and $A_{\text{free}} = 0.170 \cdot 10^4 \text{ cm} \cdot \text{mmol}^{-1}$ ($T = 206 \text{ K}$) we have $\Delta m = -0.4 \text{ kcal} \cdot \text{mol}^{-1}$, i.e. intermolecular hydrogen bonds in liquid H_2Se are weaker than those in H_2S . The high relative strength of the $2\nu_{\text{str}}$ band of H_2Se and its much higher solubility in liquid Kr (as compared to H_2S)⁵⁶ confirm this conclusion.

Just as in the case of the above-considered hydrides of Group IV-V elements, the IR spectra of chalcogenohydrogens are now better understood than the Raman spectra, and this is especially true for hydrogen selenide. Some paper are available devoted to the study of Raman spectra of hydrogen sulfide in the gas phase^{57,58} and hydrogen selenide in the solid state.⁵⁹ Spectra of H_2S in the liquid phase were studied in Ref. 58 and 60. The frequencies of fundamental vibrations in the Raman spectra of H_2S and H_2Se in the gas and liquid phases are tabulated in Table 9.

The data of the table show that, similarly to vibration spectra of hydrides of Group IV-V elements and to the IR spectra of H_2S and H_2Se , the line of

stretching vibrations, which is a superposition of ν_1 and ν_3 lines unresolved under experimental conditions, noticeably shifts toward lower frequencies at the gas-liquid transition. The frequencies of the bending vibrational lines remain practically unchanged. Analysis of ν_2 shape in the Raman spectrum of liquid hydrogen sulfide at the temperature from 188 to 295 K has shown that the contour of this line is of rotational origin. Besides, unlike other hydride molecules considered above, the H_2S molecules change their orientation stepwise. The time behavior of the obtained correlation functions of vibrational and rotational relaxation, the values of the corresponding characteristic times of these processes, and the rotation angles of the hydrogen sulfide molecules allow the conclusion on the possibility of formation of weak associates in this liquid.

Table 9. Frequencies (ν , cm^{-1}) of fundamental lines in the Raman spectra of chalcogenohydrogenes in the gas and liquid phases

Vibrational bands	H_2S		H_2Se	
	Gas $T = 293 \text{ K}$	Liquid $T = 207 \text{ K}$	Gas $T = 293 \text{ K}$	Liquid $T = 272 \text{ K}$
ν_1	2611.2		2340.6	
ν_3	2627.1	2580.0	2355.5	2308.5
ν_2	1183.0	1179.7	1031.6	1030.0

Thus, according to the data of IR absorption spectroscopy, liquid H_2S and H_2Se are weakly associated by means of intermolecular hydrogen bonds, and the energy of H-bonds decreases in the order: $\text{H}_2\text{O}-\text{H}_2\text{S}-\text{H}_2\text{Se}$.

8. Conclusion

The investigation of IR absorption spectra of gaseous molecules allows the information on their structure and molecular dynamics to be obtained. The transition to the liquid phase gives some additional information on the liquids structure and the character of intermolecular interactions under conditions of high-density ensemble of molecules. As is seen from the above consideration, the unique capabilities of the experimental setup allow not only obtaining the specifically spectroscopic (and very important) information about the structure of liquids and molecular dynamics in a wide temperature range, but also revealing the differences in the mechanisms of intermolecular interaction in these liquids.

The investigation of IR absorption spectra of liquid hydrides of Group IV–VI elements is also interesting from another point of view. As is seen from the temperatures of phase transitions for the hydrides presented in Table 2, these substances may be considered as cryogenic solvents. The disadvantage of liquid hydrides as solvents is their strong absorption in the mid-IR. On the other hand, these solvents can exist in the liquid state up to the

temperature higher than the room temperature (except for SiH_4). Their high chemical reactivity can be considered as both a merit and demerit. Solutions of liquid hydrides in wide temperature range can serve for studying various chemical processes with participation of dissolved substances with concentration of 1–3% and lower. The data available on the absorption spectra of liquid hydrides allow us to use the method of IR spectroscopy in quantitative analysis. For example, detection of CO_2 impurities in SiH_4 and GeH_4 was reported in Ref. 26, while Ref. 16 reported detection of CH_4 , CO_2 , N_2O , and H_2O in PH_3 , and Refs. 61 and 62 reported detection of CS_2 in liquid H_2S and H_2O in liquid hydrides of Group V–VI elements, respectively.

Thus, investigation of the processes of IR radiation absorption by volatile inorganic hydrides of Group IV–VI elements in the liquid state and in liquefied gas solutions is the important field of molecular spectroscopy, which develops its cryogenic direction. The information obtained therewith is of interest in studying the reactivity of inorganic hydrides, their deep purification, and analysis.

References

1. G.G. Devyatykh and A.D. Zorin, *Volatile Ultra-Pure Inorganic Hydrides* (Nauka, Moscow, 1974).
2. D.G. Tuck, in: *Comprehensive Organometallic Chemistry*, ed. by G.W. Wilkinson (Pergamon Press, New York, 1982), Vol. 1, p. 683.
3. Sh.Sh. Nabiev and Yu.N. Ponomarev, *Atmos. Oceanic Opt.* **11**, No. 12, 1093–1098 (1998).
4. G. Herzberg, *Infrared and Raman Spectra of Polyatomic Molecules* (Van Nostrand, New York, 1945).
5. L.A. Pugh and K.N. Rao, in: *Molecular Spectroscopy. Modern Research* (Academic Press, New York, 1976), Vol. 2, p. 165.
6. G.Di. Lonardo, L. Fuzina, and J. Johns, *J. Mol. Spectrosc.* **104**, 282 (1984).
7. P.G. Sennikov, D.A. Raldugin, Sh.Sh. Nabiev, V.A. Revin, and B.S. Khodzhev, *Spectrochim. Acta* **52A**, 453 (1996).
8. I. n. Bulanin, ed., *Molecular Cryospectroscopy* (St. Petersburg State University Publishing House, St. Petersburg, 1993), 300 pp.
9. Sh.Sh. Nabiev, *Izv. Ros. Akad. Nauk, Ser. Khimiya*, No. 4, 560 (1998).
10. M. Moscovits and G.A. Ozin, eds., *Crychemistry* (Wiley & Sons, New York, 1976).
11. V.D. Klimov, A.V. I amchenko, Sh.Sh. Nabiev, and L.P. Sukhanov, *Russ. J. Phys. Chem.* **65**, 966 (1991).
12. V.E. Shkrinin, L.A. Efimychev, P.G. Sennikov, and K.G. Tokh=dze, *Vysokochistye Veshchestva*, No. 6, 221 (1988).
13. S.I. I elikova, *Zh. Prikl. Spektrosk.* **45**, 515 (1986).
14. P.G. Sennikov, D.A. Raldugin, V.E. Shkrinin, and K.G. Tokh=dze, *Vysokochistye Veshchestva*, Nos. 5–6, 107 (1992).
15. Sh.Sh. Nabiev and V.D. Klimov, *Mol. Phys.* **81**, 395 (1994).
16. V.A. Kondaurov, S.I. I elikova, Sh.Sh. Nabiev, P.G. Sennikov, D.A. Raldugin, and D.N. Shchepkin, *Vysokochistye Veshchestva*, No. 3, 119 (1993).
17. A.G. I orachevskii and I.B. Sokolov, *Physical-Chemical Properties of Inorganic Molecular Compounds* (Khimiya, Leningrad, 1987), 188 pp.
18. M.O. Bulanin, *J. Mol. Struct.* **19**, 59 (1973).

19. J. Hawranek, P. Neelakemtan, R. Yang, and R. Jones, *Spectrochim. Acta* **32A**, 111 (1976).
20. I. Kessler, *Methods of Infrared Spectroscopy in Chemical Analysis* (Geest & Portig, Leipzig, 1961).
21. G.S. Denisov and B.S. Terushkin, *Molecular Spectroscopy*, (Leningrad State University Publishing House, Leningrad, 1981), Issue 5, p. 232.
22. R. Yuga and Yu. Khaldna, *Zh. Analit. Khim.* **43**, 1564 (1988).
23. L.A. Pugh and K.N. Rao, in: *Molecular Spectroscopy. Modern Research* (Academic Press, New York, 1976), Vol. 2, p. 165.
24. L. Halonen and M.S. Child, *Comput. Phys. Comm.* **57**, 173 (1988).
25. R. Bregier and P. Lepage, *J. Mol. Spectrosc.* **45**, 450 (1973).
26. P.G. Sennikov, B.E. Shkrunin, S.M. Melikova and Yu.A. Lebedeva, *Vysokochistye Veshchestva*, No. 2, 127 (1992).
27. G.P. Wilkinson and M.K. Wilson, *J. Chem. Phys.* **44**, 3867 (1996).
28. D.F. Ball and D.C. McKean, *Spectrochim. Acta* **18**, 1375 (1962).
29. J.W. Levin and W.T. King, *J. Chem. Phys.* **18**, 3867 (1962).
30. A.A. Chalmers and D.C. McKean, *Spectrochim. Acta* **21**, 1941 (1965).
31. J.W. Levin, *J. Chem. Phys.* **42**, 1244 (1965).
32. R. Fournier, R. Savoie, N. The, and A. Cabana, *Can. J. Chem.* **50**, 35 (1972).
33. G.G. Devyatykh, P.G. Sennikov, K.G. Tokhadze, and V.E. Shkrunin, *Vysokochistye Veshchestva*, No. 6, 21 (1988).
34. N. Kawasaki, E. Kawai, H. Sato, K. Sugai, and M. Hanabusa, *Jap. J. Appl. Phys.* **26**, 1395 (1987).
35. B. Lavorel, G. Millot, Q.L. Kou, G. Guelashvili, K. Bouzouba, P. Lepage, V.G. Tyuterev, and G. Pierre, *J. Mol. Spectrosc.* **143**, 35 (1990).
36. N.D. The, J.-M. Gagnon, R. Berzile, and A. Cabana, *Can. J. Chem.* **52**, 327 (1974).
37. Sh. Nabiev, I. Ostroukhova, N. Revina, L. Palkina, P. Sennikov, and D. Raldugin, in: *Abstr. of Reports at the XIIth Intern. Symp. and School on High Resolution Molec. Spectrosc.*, Petergof (1996), p. 88.
38. Sh.Sh. Nabiev and I.I. Ostroukhova, *J. Fluor. Chem.* **58**, 287 (1992).
39. Sh.Sh. Nabiev and I.I. Ostroukhova, *Vysokochistye Veshchestva*, No. 5, 121 (1993).
40. Sh.Sh. Nabiev, I.I. Ostroukhova, N.V. Revina, and L.P. Sukhanov, *Izv. Akad. Nauk, Ser. Khimiya*, No. 5, 961 (1997).
41. G.G. Devyatykh, P.G. Sennikov, and Sh.Sh. Nabiev, *Izv. Akad. Nauk, Ser. Khimiya*, No. 4, 629 (1999).
42. Sh.Sh. Nabiev, P.G. Sennikov, B.G. Sartakov, I.I. Ostroukhova, N.V. Revina, V.F. Serik, and E.V. Yashina, *Russ. J. Inorg. Chem.* **44**, No. 8 (1999).
43. A.N. Marten, *J. Chem. Phys.* **66**, 3117 (1977).
44. C. Suzer and L. Andrews, *J. Chem. Phys.* **87**, 5131 (1987).
45. Sh.Sh. Nabiev, P.G. Sennikov, D.A. Raldugin, V.A. Revin, and B.S. Khodjiev, *Vysokochistye Veshchestva*, No. 2, 22 (1994).
46. J.E. Del Bene, *J. Comput. Chem.* **10**, 603 (1989).
47. M.J. Frisch, J.A. Pople, and J.E. Del Bene, *J. Phys. Chem.* **89**, 3664 (1985).
48. I.S. Perelygin and A.S. Krauze, *Opt. Spektrosk.* **81**, 929 (1996).
49. V.I. Starikov and V.I.G. Tyuterev, *Intramolecular Interactions and Theoretical Methods in Spectroscopy of Nonrigid Molecules* (Publishing House of the Siberian Branch of the Russian Academy of Sciences, Tomsk, 1997), 230 pp.
50. G.G. Devyatykh, P.G. Sennikov, K.G. Tokhadze, and V.E. Shkrunin, *Dokl. Akad. Nauk SSSR* **309**, 638 (1989).
51. P.G. Sennikov, V.E. Shkrunin, and K.G. Tokhadze, *Vysokochistye Veshchestva*, No. 1, 183 (1991).
52. P.G. Sennikov, D.A. Raldugin, V.E. Shkrunin, and K.G. Tokhadze, *J. Mol. Struct.* **219**, 203 (1990).
53. P.G. Sennikov, *J. Phys. Chem.* **98**, 4973 (1994).
54. A.V. Iogansen, in: *Hydrogen Bond*, ed. by N.D. Sokolov, (Nauka, Moscow, 1982), p. 112.
55. D. Schioberg, C. Buanam-Om, and W.A.P. Luck, *Spectrosc. Lett.* **12**, 83 (1971).
56. P.G. Sennikov, V.E. Shkrunin, and K.G. Tokhadze, *J. Mol. Liquids* **46**, 29 (1990).
57. H. Frinder, R. Angstl, D. Illig, H.W. Schretter, L. Lechuga-Fossat, J.-M. Flaud, C. Camy-Peyret, and W.F. Murhy, *Can. J. Phys.* **63**, 1189 (1985).
58. F. Salmoun, J. Dubessy, Y. Garrabos, and F. Marsault-Herail, *J. Raman Spectrosc.* **25**, 281 (1994).
59. B. Paldus, S.A. Schlueter, and A. Andersen, *J. Raman Spectrosc.* **23**, 87 (1992).
60. V. Mazzacuraty, M. Ricci, G. Ruocco, and M. Maradone, *J. Mol. Phys.* **50**, 1083 (1983).
61. D.A. Raldugin, P.G. Sennikov, K.G. Tokhadze, and R.I. Sharibdjanov, *Vysokochistye Veshchestva*, No. 1, 33 (1989).
62. G.G. Devyatykh and P.G. Sennikov, *Uspekhi Khimii* **64**, 872 (1995).